Electrostatic Charging and Arc Discharges on Satellite Dielectrics Simulated by Electron Beam

Haruhisa Fujii,* Yoshikazu Shibuya†
Mitsubishi Electric Corporation, Amagasaki, Hyogo, Japan
Toshio Abe,‡ Ritaroh Kasai§
Mitsubishi Electric Corporation, Kamakura, Kanagawa, Japan
and
Hironobu Nishimoto¶
National Space Development Agency of Japan, Tsukusa, Ibaraki, Japan

This paper describes the electrostatic charging and discharge phenomena of dielectric materials for spacecraft by electron-beam irradiation simulating the hot plasma in space. Thermal control materials were used as the dielectrics tested. Charge accumulation in the dielectric irradiated with the partially penetrating mono-energetic electron beam causes a large potential on the surface. When the large surface potential reaches a critical value, arc discharge occurs. The rate of occurrence of the discharge increases with the electron energy and the electron-beam current density. The characteristics of the discharges, however, depend on the material.

Nomenclature

A = electron-irradiated area of the sample
C = capacitance
d = thickness of the sample
E = electron energy
e = electronic charge
H = solar spectral intensity at Air Mass 0
I = bulk current
J_b = electron-beam current density
J_{bs} = backscattered electron current density
J_e = primary electron current density
J_l = conduction current density
J_{se} = secondary electron current density
P = pressure
R = penetration depth of electron
R_e = hemispherical spectral reflectance
t = time
T_i = electron-beam irradiation time
V_s = surface potential
α_s = solar absorptance
ϵ = emittance
λ = wave length

Introduction

TODAY many satellites, for instance, communication satellites, broadcasting satellites, and geometeorlogical satellites, are in Earth orbits. These satellites must function in a tenuous charged-particle space environment. Normally, this is not hazardous, but, under certain conditions, the charged-particle environment can affect the performance of these systems profoundly. A satellite immersed in an ambient plasma will come into an electrical equilibrium with the plasma by developing surface charges on the satellite to reduce the net current between the satellite and the plasma to zero.[1-3] In sunlight conditions, the photoelectron emission from the sunlit surfaces must be sufficient to maintain the lower spacecraft potential relative to the space potential. However, there can be shaded insulator surfaces on the satellite. So, it seems that a geostationary satellite could encounter a hot plasma (or geomagnetic substorm) and become differentially charged; that is, the potentials of the shaded insulators relative to the electrical ground surfaces of the satellite would be multikilovolts negative. This phenomenon is referred to as "differential charging" on the spacecraft.[1,3] If this potential difference exceeds a breakdown threshold, then a discharge will occur. This phenomenon is known to cause mulfunctions or anomalies such as the upsetting of onboard electronics or the degradation of surface materials.[1,3] These effects must be minimized for the sake of a higher reliability and a longer operational life of the spacecraft system.

Among the charged particles in space, it is electrons that have a large influence on the electrostatic charging of spacecraft. The electron-beam irradiation method has been used to investigate the electrostatic charging and discharge phenomena of the satellite's dielectric materials, especially under the conditions simulating geomagnetic substorm.[4-6] This method has been useful for understanding the processes of the differential charging phenomena and obtaining the basic data for the development of the technologies to control the detrimental spacecraft-environment interactions.

In this paper, the charging and discharge phenomena induced by electron beams are investigated in detail for several thermal control materials.

Experiment

Figure 1 shows the schematic diagram of the experimental setup. One ~57 mm diam sample was set on the sample holder. Then the vacuum chamber was evacuated by the oil-free evacuating systems (sorption pumps and ion pumps). When the pressure in the chamber reached a level on the order of 1×10^{-6} Torr, the sample was irradiated with the mono-energetic electron beam. The electron beam was controlled at any energy level between 20 keV and 45 keV, and at any

Presented as Paper 86-1191 at the AIAA 3rd Space Systems Technology Conference, San Diego, CA, June 9-12, 1986; received Sept. 12, 1986; revision received July 27, 1987.

*Assistant Manager, Manufacturing Development Laboratory, Member AIAA.
†Manager, Manufacturing Development Laboratory.
‡Assistant Manager, Kamakura Works.
§Manager, Kamakura Works.
¶Assistant Senior Engineer, Tsukuba Space Center.

current density between 0.1 nA/cm^2 and 16 nA/cm^2. The electron-bombarded area of each sample was 19.6 cm^2 (50 mm$^\phi$).

Because of the electron-beam irradiation, the currents flow through the sample (bulk current) and along the surface of the sample (surface current). The bulk current was measured by electrometer (Advantest TR-84M) and the surface current was released to the grounded sample holder. The charging surface potential of the sample was measured by a noncontacting electrostatic voltmeter with an electrostatic probe (TREK, Inc., 340HV and 4031S).

The broken lines in Figure 1 show the measuring position of the electrostatic probe, which was moved by the rotation mechanism installed on the vacuum chamber. The gap length between the sensing aperture of the probe and the surface of the sample was about 6 mm. The photographs of the lights of arc discharges that occurred during the electron-beam irradiation were taken through the quartz window of the vacuum chamber when necessary. All the experiments were done at room temperature (about 20°C). The following thermal control materials were used as samples: silvered Teflon (FEP; fluorinated ethylene-propylene copolymer); aluminized Kapton (polyimide); and optical solar reflector (OSR).

III. Results of Experiment

Silvered Teflon

Silvered Teflon samples tested were of 1 mil (=25 μm) and 5 mil (=127 μm) thickness. First, the results of the experiment will be described in the case of silvered Teflon of 5 mil thickness.

Figure 2 shows the electrostatic charging and discharge characteristic of 5 mil silvered Teflon caused by electron-beam irradiation under the condition $E=30$ keV and $J_b=0.68$ nA/cm^2, during $T_i=60$ min. The time dependences of the bulk current through the sample, the surface potential, and the pressure, are shown in Fig. 2. This figure indicates the following:

1) After the beginning of the electron-beam irradiation, the bulk current decreased rapidly and then tended to establish a constant value with time.

2) The surface potential (negative) increased rapidly and then had a tendency to become saturated.

3) A discharge occurred at 32.2 min. At the time, a positive current pulse was imposed on the bulk current following a rapid increase, and the surface potential became near 0 V.

4) At the occurrence of the discharge, an instantaneous increase of the pressure was simultaneously observed.

5) The behaviors of the bulk current and the surface potential after the discharge were similar to those before the discharge.

The discharge frequency was found to change according to the electron energy and the beam current density. Figure 3a shows the time dependence of the cumulative number of discharges that occurred in 5 mil silvered Teflon under the condition E = 40 keV. The cumulative number of discharges is likely to increase linearly with time so that discharge frequency can be obtained from each slope of the characteristics. In Fig. 3b, the discharge frequency is plotted as a function of J_b, which indicates that the discharge frequency increases with the beam current density. Figure 4 also shows the dependence

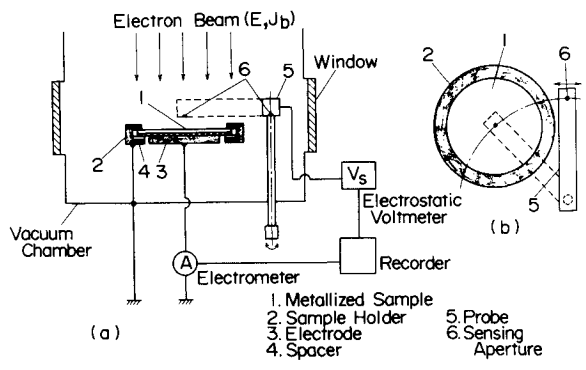

Fig. 1 Schematic diagram of experimental setup.

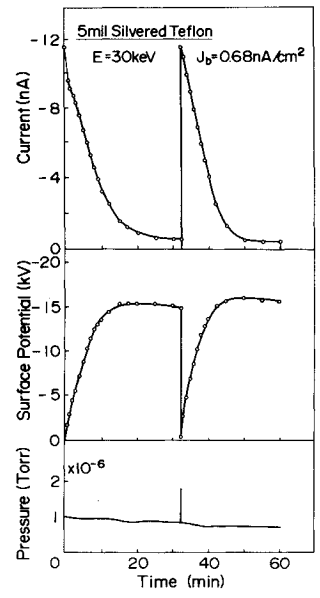

Fig. 2 Charging and discharge characteristic of 5 mil silvered Teflon at $E=30$ keV and $J_b=0.68$ nA/cm^2.

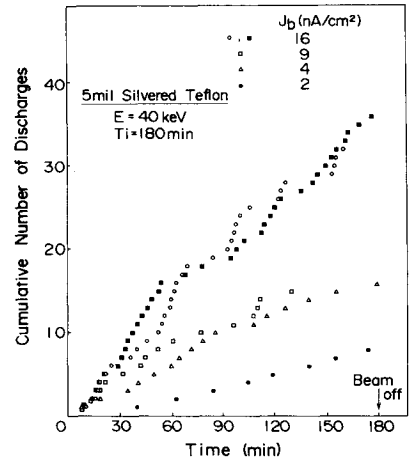

a)

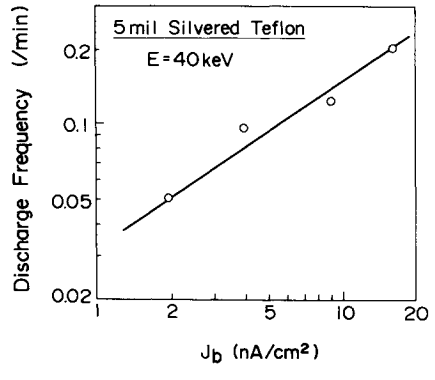

b)

Fig. 3 Discharge characteristics in 5 mil silvered Teflon at $E=40$ keV: a) Cumulative number of discharges vs time; b) Discharge frequency vs beam current density.

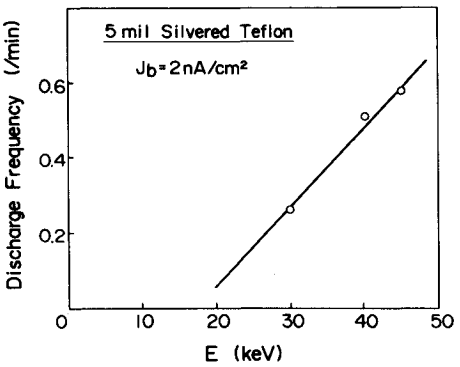

Fig. 4 Dependence of the discharge frequency on the electron energy in 5 mil silvered Teflon at $J_b = 2$ nA/cm^2.

Fig. 5 Photograph of one arcing discharge observed on 5 mil silvered Teflon.

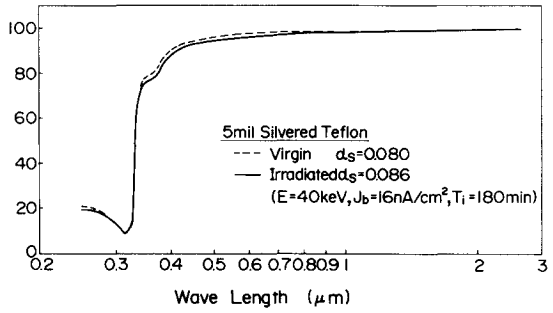

Fig. 6 Hemispherical spectral reflectances and solar absorptances of 5 mil silvered Teflons.

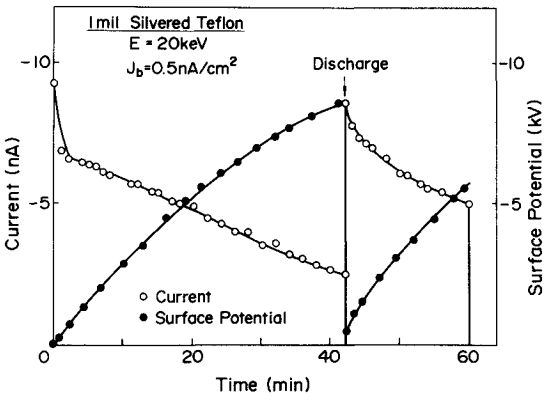

Fig. 7 Charging and discharge characteristic of 1 mil silvered Teflon at $E = 20$ keV and $J_b = 0.5$ nA/cm^2.

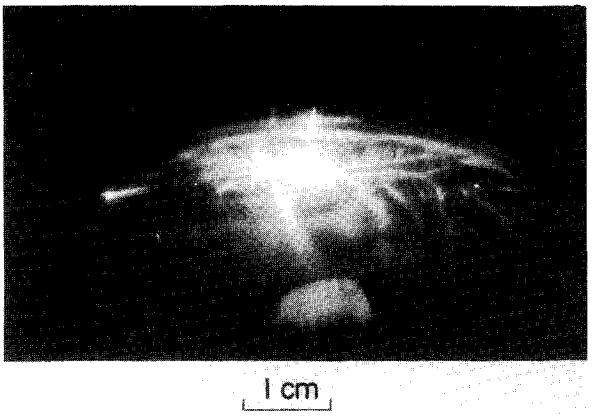

Fig. 8 Photograph of the arcing discharge observed at 42.1 min in Fig. 7.

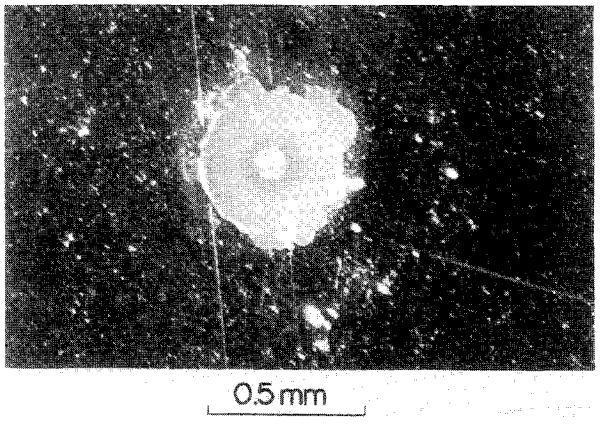

Fig. 9 Photograph of the punchthrough spot of 1 mil silvered Teflon.

of the discharge frequency on the electron energy under the condition $J_b = 2$ nA/cm2 (in the case of $E = 20$ keV, however, no discharge occurred during $T_i = 180$ min). This figure indicates that the discharge frequency increases linearly with the electron energy, but a minimum energy level seems to exist.

The discharges observed in the case of 5 mil silvered Teflon occur on the surface, as seen in the photograph of Fig. 5. On the surface of the sample where arc discharges occurred, the discharge tracks were also observed, as reported by Balmain et al.[7] From Fig. 5, it is thought that flashovers occur on the 5 mil silvered Teflon surface. For the 5 mil silvered Teflon samples that were irradiated with the electrons and discharged frequently, degradation of the solar absorptance (α_s), the important property of the thermal control material, is observed. Figure 6 shows the hemispherical spectral reflectances of the virgin sample and the irradiated sample with the electron beam of $E = 40$ keV and $J_b = 16$ nA/cm2 during 180 min. It is found that in the irradiated sample the reflectance in the ultraviolet and visible regions lowers and α_s, calculated from this spectral reflectance using Eq. (1) (λ in unit of μm), increases.

$$\alpha_s = 1 - \int_{0.25}^{2.5} R_e(\lambda) H(\lambda) d\lambda \Big/ \int_{0.25}^{2.5} H(\lambda) d\lambda \qquad (1)$$

However, emittance (ϵ), the other important property, does not deteriorate, even in the irradiated sample shown in Fig. 6.

Next, the characteristics of the electron-beam irradiated, 1 mil silvered Teflon, are described. Figure 7 shows the time dependences of the bulk current and the surface potential of 1 mil silvered Teflon subjected to the beam of $E = 20$ keV and $J_b = 0.5$ nA/cm^2. The resulting characteristic is quite similar

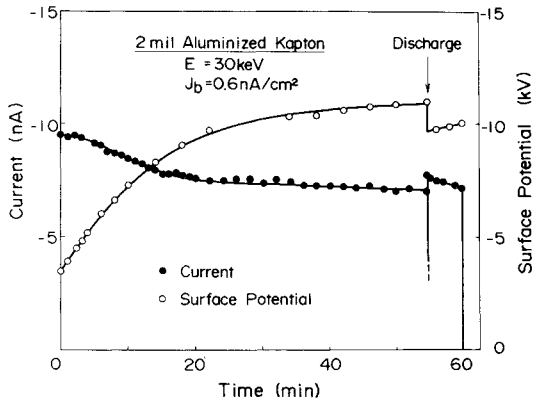

Fig. 10 Charging and discharging characteristic of 2 mil aluminized Kapton at $E = 30$ keV and $J_b = 0.6$ nA/cm^2.

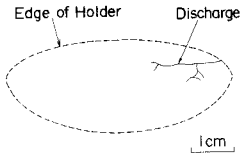

Fig. 11 Sketch of the discharge occurred at 54 min in Fig. 10.

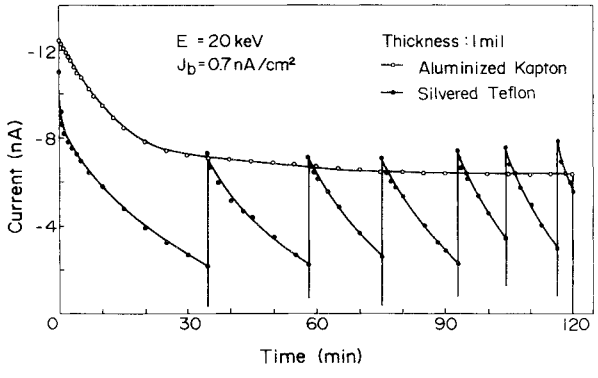

Fig. 12 Bulk currents as a function of time in aluminized Kapton and silvered Teflon of the thickness of 1 mil.

to that of 5 mil silvered Teflon shown in Fig. 2. The light of the arcing discharge observed at 42.1 min, which is shown in the photograph of Fig. 8, is, however, different from that of 5 mil silvered Teflon (Fig. 5). The morphology of the discharge has a bright spot near the center of the sample and the discharge branches toward the bright spot. Figure 9 also shows the portion where the bright spot was observed. From this photograph, a 30 μm diam hole is observed, and the deposited silver of the back surface surrounding the hole is found to be peeled off.[8] Therefore, we believe that the discharge occurring in the case of the 1 mil silvered Teflon is the punchthrough accompanying the flashover on the surface.

Aluminized Kapton

We also investigated the electron-beam induced charging and discharge characteristics of aluminized Kapton. Figure 10 shows one example of the time dependences of the bulk current and the surface potential of 2 mil aluminized Kapton subjected to the beam of $E = 30$ keV and $J_b = 0.6$ nA/cm^2. This characteristic is substantially similar to those of silvered Teflon. The discharge that occurred at 54 min was, however, small and local. (Figure 11 is a sketch of the light of the discharge.) Therefore, the change of the surface potential is small. Relatively smaller discharges occur on aluminized Kapton, compared with silvered Teflon. Accordingly, the influence of the discharge occurring in the case of aluminized Kapton is thought to be smaller than that in the case of silvered Teflon.

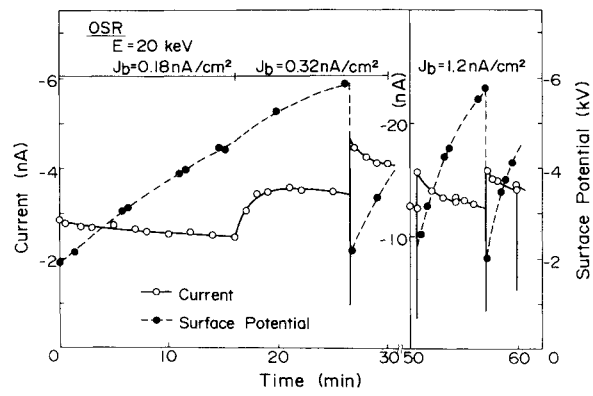

Fig. 13 Charging and discharging characteristic of a set of four OSR's at $E = 20$ keV.

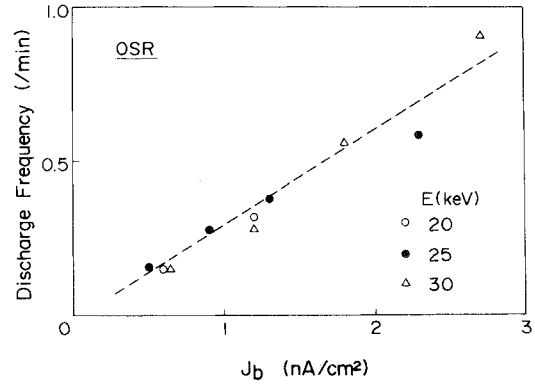

Fig. 14 Dependence of the discharge frequency on the beam current density in OSR's.

In addition, discharges occur less frequently by far in aluminized Kapton than in silvered Teflon if compared under the same conditions. As one example, in Fig. 12, the bulk currents as a function of time are shown in aluminized Kapton and silvered Teflon of the same 1 mil thickness, under the electron-beam irradiation condition of $E = 20$ keV and $J_b = 0.7$ nA/cm^2. During $T_i = 120$ min, no discharge occurred in the aluminized Kapton, but six major discharges occurred in silvered Teflon.

Optical Solar Reflector (OSR)

Recently, OSR has been increasingly used because of its good emittance property. We investigated the charging and discharge characteristics of OSR through electron-beam irradiation. The samples (OCLI #6065002) were square and small, 20×20 mm^2 and 8 mil thick. Four of them were placed in the sample holder.

Figure 13 shows one example of the charging and discharge characteristic of the test sample, under the condition of $E = 20$ keV. This figure indicates that discharges occur when the surface potential reaches about -6 kV. These discharges are observed to occur at the edges or in the gaps between OSR's. Figure 14 shows the dependence of discharge frequency on the electron-beam current density. From this figure, it is understood that the discharge frequency increases with the beam current density, irrespective of the electron energy.

Discussion

In general, in the charging model shown in Fig. 15, the bulk current measured by the electrometer is expressed as follows:

$$I = A \cdot [J_e(E, V_s) - J_{se}(E, V_s) - J_{bs}(E, V_s)] \quad (2)$$

$$= C \cdot dV_s/dt + A \cdot J_1(V_s) \quad (3)$$

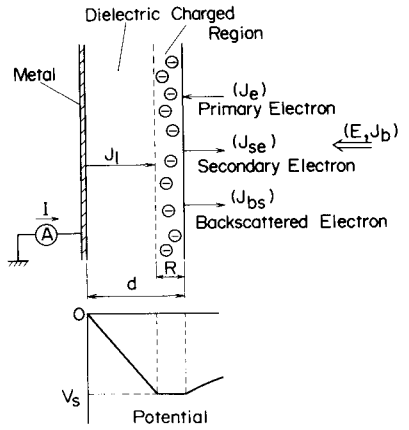

Fig. 15 Simple model of electrostatic charging due to electron-beam irradiation.

Table 1 Calculated penetration depth of electron in Teflon (FEP)

E (keV)	R (cm)
20	4.0×10^{-4}
30	8.0×10^{-4}
40	13.2×10^{-4}
45	16.1×10^{-4}

J_e, J_{se}, and J_{bs} are the functions of E and V_s, and J_1 is the function of V_s.[1,9] The incident electrons partially penetrate into the dielectric in response to the energy. The electrons are accumulated as space charges within the penetration depth, and the surface potential is built up as shown in the lower part of Fig. 15. This penetration depth is calculated by using, for example, Gledhill's relation.[10] The calculated results are shown in Table 1 in the case of Teflon (FEP).

Because the secondary electron emission yields of Teflon,[11] Kapton,[11] and fused silica SiO_2 (OSR)[12] seem to be very small in the case of the incident electron energy between 20 keV, almost all the incident electrons are accumulated in the dielectric at the initial stage of the electron irradiation. Then, from Eqs. (2) and (3), the surface potential builds up at the rate of

$$dV_s/dt = (A/C)J_e \tag{4}$$

By this buildup of the surface potential, the conduction current gradually becomes dominant. Also, the effective incident energy of the electron becomes $(E - e|V_s|)$, which leads to the increase of the secondary electron current. Therefore, the surface potential has a tendency to become saturated gradually, and the bulk current tends to a certain value after decreasing, as shown in Fig. 2 and 7 (silvered Teflon), in Fig. 10 (aluminized Kapton), and in Fig. 13 (OSR).

When these surface potentials exceed the critical values (about -15 kV in the case of 5 mil silvered Teflon), the discharges occur. By these discharges, the accumulated electrons in the dielectrics are released to the ground. In the case of the discharge in 5 mil silvered Teflon as shown in Fig. 2, the released charge is about 4.4×10^{-6} C. Also, the instantaneous increase of the pressure is observed at the occurrence of the discharge, which seems to be caused by the gasification of polymer by the discharge energy.

The morphology of the discharge in 5 mil silvered Teflon is different from that in 1 mil silvered Teflon, as seen in Fig. 5 and 8. The surface potential V_s induces the electric field in the nonpenetrating region of the dielectric. Because the penetration depths are on the order of 10 μm as shown in Table 1, the electric field induced in 5 mil silvered Teflon is nearly 1 MV/cm, even in the discharge potential. This value is considerably lower than the intrinsic dielectric strength of Teflon (FEP).[13] Therefore, surface flashover occurs more easily than intrinsic bulk breakdown (punchthrough) in 5 mil silvered Teflon. On the other hand, the electric field induced in the nonpenetrating region of 1 mil silvered Teflon is about 5 MV/cm, which is on the order of the intrinsic dielectric breakdown strength.[13] Therefore, the dielectric breakdown in the bulk, namely punchthrough discharge, occurs and triggers the surface discharge. By this discharge energy, the silver deposited on the back surface is peeled off, as seen in Fig. 9; this seems to increase solar absorptance.

Also, in the case of OSR, the potentially occurring punchthrough discharge is much higher because of the larger thickness (8 mil) and the high dielectric strength of fused silica SiO_2 (about 10 MV/cm),[14] so that the discharges occur as surface flashover at the OSR edges.

The volume resistivity of Kapton is lower than that of Teflon (FEP), so that the accumulated charges in the aluminized Kapton are easier to release through the bulk of the Kapton. Therefore, under the same irradiation condition, the discharge on aluminized Kapton seems to occur with difficulty compared to silvered Teflon.

The characteristics of discharge frequency are discussed next. In 5 mil silvered Teflon, the discharge frequency increases with the electron-beam current density. The reason is that the increase of the beam current density allows the critical potential at which the discharge occurs to be reached immediately. On the other hand, the discharge frequency increases linearly with the electron energy, but the threshold energy seems to exist. The reason seems to be as follows.

As shown in Table 1, the penetration depth of the incident electron increases with the electron energy so that the capcitance of the nonpenetrating region increases with the electron energy. Although the charge buildup speed at the initial stage of the electron irradiation with the higher energy is slower, due to the larger capacitance from Eq. (4), the charge buildup seems to reach a higher level owing to smaller secondary electron emission. So, the discharge occurs more easily in the case of the electron irradiation with higher energy. However, in the case of the lower-energy electron irradiation, the surface potential could become saturated below the discharge potential because the incident electron current balances with the larger secondary electron emission current. Therefore, the threshold energy exists in the dependence of the discharge frequency on the electron energy.

In OSR, the discharge frequency is found to increase with the beam current density, irrespective of the electron energy. The electron energy has no remarkable effect on the capacitance of nonpenetrating region because of larger thickness (8 mil). This may be the reason why the discharge repetition rate of OSR is indifferent to the electron energy in contrast to the result of 5 mil silvered Teflon.

Elimination of Electrostatic Charging

One method to eliminate the electrostatic surface charging of the dielectric as described above is to make the dielectric surface electrically conductive. Because thermal control materials must have the thermo-optical properties α_s and ϵ, it is not appropriate to coat the surface with deposited metal. It is necessary to apply transparent conductive coatings on the surfaces, for example, IO (Indium Oxide) and ITO (Indium Tin Oxide). In order to test the effect of the transparent conductive coating on the surface charging of the dielectric, we investigated the charging characteristic of 1 mil aluminized Kapton coated with a thin IO layer (Sheldahl Inc. # G410610) by irradiating it with the electron beam in the experimental setup as shown in the insert of Fig. 16.

Figure 16 shows the time dependences of the bulk current, the surface current, and the surface potential under the condition of $E = 30$ keV (J_b was increased at a time interval of 30 min). The very low measured surface potentials, less than 100 V, indicate that the surface charging is negligible. Also, the surface current proportional to the electron-beam current

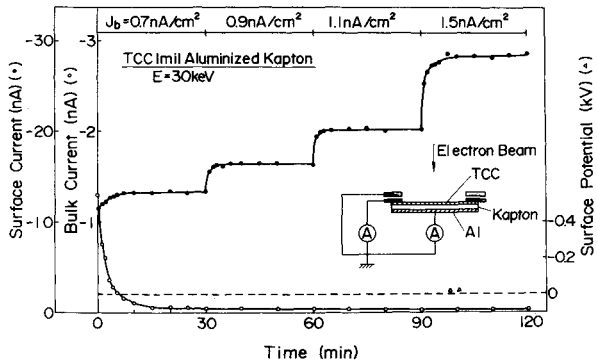

Fig. 16 Time dependences of the bulk current, the surface current, and the surface potential of transparent conductive coating (TCC) aluminized Kapton at $E = 30$ keV.

density indicates that the major part of the injected electron current flows as the surface current. From this result, it was confirmed that the transparent conductive coating on the thermal control material effectively eliminates the electrostatic surface charging.

Concluding Remarks

We simulated the electrostatic charging and discharging on the satellite surface materials by means of electron-beam irradiation. The results obtained are as follows:

1) Silvered Teflon is found to be more vulnerable to the electrostatic charging than aluminized Kapton.

2) Two types of discharges exist in silvered Teflon. One is the surface flashover in the case of the thick samples, and the other is the punchthrough discharge accompanying the surface flashover in the case of the thin samples.

3) The discharge frequency increases with the electron energy and the electron-beam current density for silvered Teflon.

4) The discharges cause the solar absorptance of thermal control material to deteriorate in the case of silvered Teflon.

5) In OSR, discharges are likely to occur at the joining edges.

6) Coating the conductive thin layer on the dielectric surface is effective as a countermeasure to the electrostatic charging.

Acknowledgments

The authors would like to thank Dr. Shoji Hirabayashi, Fumihiko Sato and Katsutoshi Ohmura of MELCO for their steady encouragements. Useful technical discussions with Dr. Tadashi Matsushita and Hiroyoshi Yamada of NASDA, and Tsutomu Tani and Dr. Koichiro Nakanishi of MELCO, are gratefully acknowledged.

References

[1]Garrett, H.B., "The Charging of Spacecraft Surfaces," *Reviews of Geophysics and Space Physics,* Vol. 19, Nov. 1981, pp. 577-616.

[2]Francis, C.R., "Electrostatic Charging Problems of Spacecraft," *Journal of Electrostatics,* Vol. 11, Feb. 1982, pp. 265-280.

[3]Grard, R.J.L., Knott, K., and Pedersen, A., "Spacecraft Charging Effects," *Space Science Reviews,* Vol. 34, March 1983, pp. 289-304.

[4]Stevens, N.J., Berkopec, F.D., Staskus, J.V., Bleck, R.A., and Narciso, S.J., "Testing of Typical Spacecraft Materials in a Simulated Substorm Environment," *Proceedings of the Spacecraft Charging Technology Conference,* edited by C.P. Pike and R.R. Lovell, NASA TMX-73537/AFGL-TR-77-0051, 1977, pp. 431-457.

[5]Leung, M.S. and Kan, H.K.A., "Laboratory Study of the Charging of Spacecraft Materials," *Journal of Spacecraft and Rockets,* Vol. 18, Dec. 1981, pp. 510-514.

[6]Verdin, D., "Electrostatic Charging of Spacecraft Materials," *Journal of Electrostatics,* Vol. 11, Feb. 1982, pp. 249-263.

[7]Balmin, K.G. and Dubois, G.R., "Surface Discharges on Teflon, Mylar and Kapton," *IEEE Transactions on Nuclear Science,* Vol. NS-26, Dec. 1979, pp. 5146-5151.

[8]Yadlowsky, E.J. and Hazelton, R.C., "Studies of Microdamage in Dielectric Discharges," *Journal of Spacecraft and Rockets,* Vol. 22, June 1985, pp. 282-286.

[9]Purvis, C.K., Stevens, N.J., and Olgebay, J.C., "Charging Characteristics of Materials: Comparison of Experimental Results with Simple Analytical Models," *Proceedings of the Spacecraft Charging Technology Conference,* edited by C.P. Pike and R.R. Lovell, NASA TMX-73537/AFGL-TR-77-0051, 1977, pp. 459-486.

[10]Gross, B., "Radiation-Induced Charge Storage and Polarization Effects," *Electrets,* edited by G.M. Sessler, Springer-Verlag, Berlin, 1980, pp. 217-284.

[11]Willis, R.F. and Skinner, D.K., "Secondary Electron Emission Yield Behaviour of Polymers," *Solid State Communications,* Vol. 13, Sept. 1973, pp. 685-688.

[12]Vigouroux, J.P., Lee-Deacon, O., Le Gressus, C., Juret, C., and Boizian, C., "Surface Processes Occurring during Breakdown of High-Voltage Devices," *IEEE Transactions on Electrical Insulation,* Vol. EI-18, June 1983, pp. 287-291.

[13]Jolley, C.E., Hamsy, C.A., and Reed, J.C., "Thermoplastics. TFE-FEP Fluorocarbons," *Machine Design,* Vol. 36, 1964, p. 67.

[14]O'Dwyer, J.J., *The Theory of Electrical Conduction and Breakdown in Solid Dielectrics,* Clarendon Press, Oxford, U.K., 1973, pp. 276-278.